FIFTH AUSTRALASIAN CONFERENCE

on

HYDRAULICS AND FLUID MECHANICS

at

University of Canterbury, Christchurch, New Zealand
1974 December 9 to December 13

THE NUMERICAL SOLUTION OF BLADE-TO-BLADE TURBOMACHINE FLOWS USING A MATRIX METHOD.

by

R.S. BENSON, M.J. HILL and W.G. CARTWRIGHT

SUMMARY

A solution procedure is presented for the two-dimensional equations of steady, adiabatic, inviscid flow on a blade-to-blade surface of revolution, in a rotating coordinate system. An analysis of compressible (or incompressible) flow through any configuration of turbomachinery blading is possible, and this may include multiple sets of splitter and tandem blades. The application may be for axial, radial or mixed flow through stators, rotors or plane cascades.

The two-dimensional flow equations are formulated in terms of stream function and then reduced to an algebraic form by using finite-difference approximations. The resulting non-linear set of simultaneous equations is solved on a fixed orthogonal grid using an iterative matrix solution technique. In order to accommodate both high speed and low speed flows, it is found to be highly desirable to incorporate convergence criteria for both stream function and density. Convergence is achieved without the use of a damping factor.

The numerical techniques have been used to analyse flows through a wide range of turbomachinery applications and a cross-section of the results obtained are presented and compared with calculations and experiments published elsewhere.

R.S. Benson, Professor of Mechanical Engineering
M.J. Hill, Special Research Assistant
W.G. Cartwright, Senior Lecturer in Mechanical Engineering

University of Manchester Institute of Science & Technology, Manchester England.

1. INTRODUCTION.

The general two-dimensional equations for flow on a blade-to-blade surface are well formulated, but the various solution procedures used for these equations differ in the mathematical and numerical techniques employed. Many of these solution procedures have particular limitations, e.g., incompressible flow, or may be restricted to certain turbomachine geometries. Of the more general procedures available, some are unable to provide solutions at even moderately high subsonic Mach numbers, and many require repeated reruns to obtain suitable damping or relaxation factors.

A new solution procedure has been formulated by Hill (1)* which can be used for all subsonic flow applications on the blade-to-blade surface of any turbomachine. The resulting computational technique, which is written in ASA FORTRAN IV (a full program listing is included in reference 1), has been used to analyse a wide variety of turbomachine geometries and flow conditions, and has so far always been successful in producing a solution without the use of any damping factor to aid convergence. In this paper, an outline to the numerical techniques is given and comparisons made with experiment and other workers' calculations.

2. NOTATION.

(A) band matrix used in fixed grid solution
a_T flow area at rotor tip defined as $2\pi r_T h_T$
c_o absolute stagnation speed of sound upstream
h passage height
H passage height ratio defined as h/h_T
m meridional coordinate
$\dot{m}$ total flow rate through rotor
M meridional coordinate ratio defined as m/r_T
nb number of blades
p static pressure
P a parameter defined by equation (25)
Q a constant at each grid point defined by equation (24)
r radius from axis of rotation
R radius ratio, r/r_T, for analytical section
s percentage blade surface length
s_1, s_2, t_1, t_2 finite difference molecule arm-lengths
U_T non-dimensional blade tip speed defined as $r_T\omega/c_o$
w relative velocity
W relative velocity ratio defined as w/c_o
$\underline{y}$ right-hand side vector used in fixed grid solution
z axial coordinate
α angle between tangent to meridional line and axis of rotation
λ whirl ratio defined as $R(RU_T + W_\theta)$
κ ratio of specific heats
ρ fluid density
ψ stream function
ψ_n stream function value corresponding to the total flow through one blade configuration
$\underline{\psi}$ vector of stream function values
θ angular coordinate
ω angular velocity

Subscripts

M meridional component
o absolute upstream stagnation condition
T rotor tip property
θ tangential component

*Numbers in parentheses designate References listed in Section 9.

3. BASIC EQUATIONS.

The basic equations of motion, energy and continuity for a two-dimensional inviscid flow on a surface of revolution in an M-θ coordinate system (figure 1) are given by:-

$$\frac{1}{R^2}\frac{\partial^2\psi}{\partial\theta^2} + \frac{\partial^2\psi}{\partial M^2} + \left(\frac{\sin\alpha}{R} - \frac{1}{H}\frac{\partial H}{\partial M}\right)\frac{\partial\psi}{\partial M}$$

$$= 2\,U_T\,H\,\frac{\rho}{\rho_o}\sin\alpha + \frac{1}{(\rho/\rho_o)}\,\frac{\partial(\rho/\rho_o)}{\partial M}\,\frac{\partial\psi}{\partial M} + \frac{1}{R^2(\rho/\rho_o)}\,\frac{\partial(\rho/\rho_o)}{\partial\theta}\,\frac{\partial\psi}{\partial\theta} \qquad (1)$$

$$\frac{\rho}{\rho_o} = \left[1 + \frac{\kappa-1}{2}\left(\left(R\,U_T\right)^2 - W^2 - 2\,U_T\lambda\right)\right]^{\frac{1}{\kappa-1}} \qquad (2)$$

$$W\,\frac{\rho}{\rho_o} = \left(\left(\frac{1}{HR}\frac{\partial\psi}{\partial\theta}\right)^2 + \left(\frac{1}{H}\frac{\partial\psi}{\partial M}\right)^2\right)^{\frac{1}{2}} \qquad (3)$$

where the derivatives of the stream function satisfy

$$\frac{\partial\psi}{\partial\theta} = \frac{\rho}{\rho_o}\,HR\,W_M \qquad (4)$$

$$\frac{\partial\psi}{\partial M} = -\frac{\rho}{\rho_o}\,H\,W_\theta \qquad (5)$$

and the prewhirl λ, is given by

$$\lambda = R(RU_T + W_\theta) \qquad (6)$$

The equations (1)-(6) are in a non-dimensionalised form and equation (1) is arranged with all terms containing the density ratio ρ/ρ_o, on the right hand side. It is these forms of the equations that are used in the computer program to enable an efficient iterative technique for their solution.

The following assumptions hold for the solution of these equations:

(i) inviscid flow

(ii) adiabatic flow

(iii) the flow is steady relative to the rotating frame of reference

(iv) the stream surface is a surface of revolution and the stream sheet thickness is constant in the tangential direction

(v) the region of solution is to be chosen such that the upstream and downstream boundaries are far enough from the bodies (blades) for all fluid properties to be uniform along them.

The equations are presented in a non-dimensional form, so that any consistent set of units may be used, without the introduction of any conversion factors. The equations have been derived in an M-θ coordinate system, where M is a non-dimensionalised distance measured along the meridional surface. This choice of coordinate enables the problem to be solved for mixed-flow turbomachines with sections that are purely axial or purely radial.

4. REGION OF SOLUTION.

It is the choice of the region of solution that simplifies the whole approach to the problem and enables the flow to be computed around any number of complicated blade shapes with virtually no more difficulty than around one simple blade.

The region of solution is chosen as that part of the M-θ surface of revolution which is bounded by the two radial planes θ=0 and $\theta = \frac{2\pi}{nb}$ radians, where nb is the number of similar configurations of blading found in one complete revolution of the surface, (figure 2). The other boundaries of this finite region of solution are the lines M = constant, AB and CD (figure 2). These are chosen far enough away from the obstacles such that the flow is uniform along these boundaries.

The region of solution does not depend, therefore, on the shape of the blading, as is usual (2,3,4,5,6) but is always rectangular in the M-θ plane (figure 3). The blades are generally interior to the region, but may cross the boundaries. When a blade crosses out of the region of solution through one θ = constant boundary, then because of the periodicity of the configurations and choice of nb, the continuation of a similar blade will appear in from the other θ = constant boundary. Thus the addition of numerous blades does not complicate the region of solution, but merely requires extra internal boundary conditions.

5. BOUNDARY CONDITIONS.

Along the boundaries θ = constant of the region of solution, (figure 3) the requirement of periodicity necessitates that all fluid properties at corresponding points (i.e., similar values of meridional coordinate M) shall be the same. It also follows that the mass flow rate between every such corresponding pair of points must be the same, and therefore the difference in the stream function values of two such points is a constant, ψ_n, where

$$\psi_n = \frac{2\pi}{nb} \frac{\dot{m}}{\rho_o a_T c_o} \tag{7}$$

It is required that the upstream and downstream boundaries AB, CD have been taken some reasonable distance away from the blading in order to assume that the distribution of fluid properties is uniform along these boundaries.

Further boundary conditions are also required inside the region of solution on the blade surfaces. Since the blade surfaces are streamlines, the stream function is constant along the surface of each blade, this constant being determined by the fraction of the total mass flow required to pass between any two blades.

6. NUMERICAL PROCEDURE.

The equations (1)-(3) are solved using finite-difference techniques on a fixed grid. The region of solution is covered with an orthogonal M-θ grid and the grid-points are numbered sequentially as shown in figure 3, including those points falling inside blade surface contours. Then, starting with an initial approximation for the density ratios ρ/ρ_o and the stream function values ψ at all the grid points, the numerical method of solution is basically an iterative procedure between the solution of equation (1) for new estimates of the stream function values ψ, and calculation of new estimates for density ratio ρ/ρ_o at each grid point using equations (2) and (3).

It has been found that, in a region of the flow having low Mach numbers, the stream function estimates are particularly sensitive to small changes of density ratio in that region. Experience has also shown that if the Mach number is close to unity at some grid points, then the density ratio estimates are particularly sensitive to small changes of stream function in that region. For these reasons, it is essential that the iterative solution procedure is terminated only when both the stream function and density ratios have satisfied some predefined convergence criterion.

6.1 Solution for Stream Function.

The partial differential equation (1) can be expressed in the form:

$$\frac{\partial^2\psi}{\partial M^2} + B\frac{\partial^2\psi}{\partial\theta^2} + C\frac{\partial\psi}{\partial M} = D \tag{8}$$

where

$$B = \frac{1}{R^2} \tag{9}$$

$$C = \frac{\sin\alpha}{R} - \frac{1}{H}\frac{\partial H}{\partial M} \tag{10}$$

$$D = 2U_T H \frac{\rho}{\rho_o}\sin\alpha + \frac{1}{(\rho/\rho_o)}\frac{\partial(\rho/\rho_o)}{\partial M}\frac{\partial\psi}{\partial M} + \frac{1}{R^2\,\rho/\rho_o}\frac{\partial(\rho/\rho_o)}{\partial\theta}\frac{\partial\psi}{\partial\theta} \tag{11}$$

Using the finite-difference approximations for a five-point molecule on an orthogonal grid, (figure 4).

$$\frac{\partial\psi}{\partial M} = \frac{s_1^2\,\psi_d - s_2^2\psi_a + (s_2^2-s_1^2)\psi_o}{s_1 s_2 (s_1+s_2)} \tag{12}$$

$$\frac{\partial\psi}{\partial\theta} = \frac{t_1^2\psi_c - t_2^2\psi_b + (t_2^2-t_1^2)\psi_o}{t_1 t_2 (t_1+t_2)} \tag{13}$$

$$\frac{\partial^2\psi}{\partial M^2} = 2\left(\frac{s_2\psi_a + s_1\psi_d - (s_1+s_2)\psi_o}{s_1 s_2 (s_1+s_2)}\right) \tag{14}$$

$$\frac{\partial^2\psi}{\partial\theta^2} = 2\left(\frac{t_2\psi_b + t_1\psi_c - (t_1+t_2)\psi_o}{t_1 t_2 (t_1+t_2)}\right) \tag{15}$$

The finite-difference equation at a general grid-point is given by

$$E\psi_a + F\psi_b + G\psi_o + H\psi_c + I\psi_d = J \tag{16}$$

where

$$E = \frac{t_1 t_2 s_2}{(s_1+s_2)}\,(2-s_2 C) \tag{17}$$

$$F = \frac{2Bt_2 s_1 s_2}{(t_1+t_2)} \tag{18}$$

$$G = -2t_1 t_2 - 2Bs_1 s_2 + C(s_2-s_1)t_1 t_2 \tag{19}$$

$$H = \frac{2Bt_1 s_1 s_2}{(t_1+t_2)} \tag{20}$$

$$I = \frac{t_1 t_2 s_1}{(s_1+s_2)}\,(2+s_1 C) \tag{21}$$

$$J = D\, s_1 s_2 t_1 t_2 \tag{22}$$

These coefficients of the finite difference equation (16) are calculated at each numbered grid-point. At grid-points adjacent to the blades or the boundaries of the region of solution, some of the ψ_a, ψ_b, ψ_c and ψ_d values will be known, and the appropriate terms are transferred to the right hand side. Also, periodicity considerations will enable the ψ_b and ψ_c which fall at non-numbered grid-points to be expressed as $\psi_b - \psi_n$ or $\psi_c + \psi_n$ at numbered grid-points, with a consequent transfer of $-F\psi_n$ or $+H\psi_n$ to the right hand side. This results in a non-linear system of equations which may be written in the form:

$$(A)\,\underline{\psi} = \underline{y} \tag{23}$$

The vector $\underline{\psi}$ is the required solution for the stream function at the grid-points. The matrix (A) is a band matrix, its elements being the coefficients E, F, G, H and I of equation (16). These coefficients remain constant throughout the solution procedure, since they are functions of geometry and grid-size only. The right hand side vector $\underline{y}$ is a combination of the functions J of equation (22) and some known terms transferred from the left hand side.

The solution of the system $(A)\underline{\psi} = y$ is computed using a 'direct' procedure rather than relaxation. Only the band elements of the matrix (A) are computed and stored and the direct solution is obtained using this minimal store by a process known as the Thomas algorithm (7). By choice of the form of the original partial differential equation (1), the matrix (A) is a function of geometry and grid-size only and therefore need only be set up once. Consequently, it is just the right hand side vector $\underline{y}$ that changes each iteration and the Thomas algorithm also makes the most efficient use of this.

It will be noted that the vector $\underline{\psi}$ is solved for numbered grid-points both inside and outside the blades. In fact, the system $(A)\underline{\psi} = \underline{y}$ contains equations for points inside the blades that are decoupled from the rest of the equations. Although flow inside the blades has no physical importance, the equations are retained in the system $(A)\underline{\psi} = \underline{y}$ in order to preserve the bandwidth of the matrix (A) and to enable the use of an efficient computational procedure whatever the blade shapes.

6.2 Solution for Density Ratios.

At a particular grid point, a constant Q, is defined by

$$Q = 1 + \frac{\kappa-1}{2}\left(\left(RU_T\right)^2 - 2\,U_T\,\lambda\right) \tag{24}$$

and a parameter P, by

$$P = \left(\frac{1}{H}\frac{\partial\psi}{\partial M}\right)^2 + \left(\frac{1}{HR}\frac{\partial\psi}{\partial\theta}\right)^2 \tag{25}$$

So equation (2) may be written

$$\left(\frac{\rho}{\rho_o}\right)^{\kappa-1} = Q - \frac{\kappa-1}{2}W^2 \tag{26}$$

and equation (3) may be written

$$W^2 = \frac{P}{\left(\frac{\rho}{\rho_o}\right)^2} \tag{27}$$

Equations (26) and (27) have two solutions for density ratio $\frac{\rho}{\rho_o}$, and these solutions may both be real or both complex, depending on the values of P and Q. For a given constant Q, the condition for real solutions is

$$P \leq \left(\frac{2Q}{\kappa+1}\right)^{\frac{\kappa+1}{\kappa-1}} \tag{28}$$

and this must be tested embarking on any solution procedure. If both solutions for density ratio are real and distinct, then the larger solution corresponds to a relative Mach number less than unity, and the smaller to a relative Mach number greater than unity.

Since the solution procedure is for subsonic flow, it is the larger solution for density ratio that is sought from equations (26) and (27), and this could be found iteratively to any desired degree of accuracy. However, since the parameter, P, is only calculated from an estimate of stream function, it has been found sufficient to use a 'non-iterative' technique and simply find an approximate solution to equations (26) and (27). This is done by determining the velocity ratio, W, from equation (27) using the density ratio, ρ/ρ_o, from the previous solution, and then evaluating the new estimate for density ratio, ρ/ρ_o, from equation (26). As the solution to the whole problem converges, then this 'non-iterative' procedure for new estimates of density ratio converges to the required larger solution of equations (26) and (27).

If as sometimes happens, the current estimate of stream function produces a value of P that is too large to satisfy condition (28), then equations (26) and (27) have no real solutions. In these circumstances, the new estimate for density ratio, ρ/ρ_o, is taken as

$$\frac{\rho}{\rho_o} = \left(\frac{2Q}{\kappa+1}\right)^{\frac{1}{\kappa-1}} \tag{29}$$

This is only an interim measure to enable the solution techniques to proceed, and must not be the state of affairs when the final flow solution is assumed to have been reached.

7. COMPARATIVE CALCULATIONS WITH HILL-FIXED GRID METHOD.

A number of calculations by the new method (called the Hill Fixed Grid Method) have been carried out to compare the results with the published results produced by other methods. The comparisons cover examples taken from a wide range of turbomachine types, including axial and radial flow, compressors and turbines. In some of the examples, experimental data is available to verify the computed flow structure.

7.1 Exact Solutions.

Mathematically exact analytical solutions, obtained by transformation methods, are possible in some cases of flow through bladed regions. When a numerical computational procedure is applied to a situation where such a solution exists, an extremely valuable check on the accuracy of the computation is possible.

Gostelow (8) has given an exact solution for incompressible flow through a cascade of plane aerofoils. The deflection angle was 23.5°, the stagger angle 37.5° and the pitch/chord ratio 0.99. Full details of the geometry are given in (8). A comparison of Hill's Fixed Grid Method and Gostelow's exact solution for pressure coefficients on the blade surfaces is shown in figure 5. The results show very good agreement, except around the blade leading edge. The reason for this difference is the truncation error of Hill's method. In this leading edge region, the streamlines are highly curved, and since the finite-difference equations (12) to (15) are obtained from a truncated Taylor series, the effect of ignoring terms containing higher derivatives of stream function produces the discrepancy. However, the finer the grid-size used for the grid method, the more the discrepancy would be reduced, since the ignored terms of the Taylor series also contain powers of the grid step-lengths.

7.2 Compressible Flow Through a Turbine Stator.

Whitney et al (9) give experimental data on flow through the nozzles of a turbine for a high temperature application. Figure 6 shows the blade surface velocity distributions produced by Hill, compared with the experimental results. In general, correlation is good, particularly on the pressure surface. On the suction surface, the Hill distribution follows the trend of the experimental points but falls slightly lower for the second 50% of the surface. The discrepancy at the trailing edge is due to its high curvature and the great sensitivity of the location of the trailing edge stagnation point to small changes of outlet flow angle and blade-shape definition.

7.3 Flow in a Centrifugal Compressor with Splitter Blades.

Katsanis (4) gives the results of a numerical computation of flow through the rotor of a centrifugal compressor described by Kramer (3). Splitter blades were present at the rotor outlet, extending over the final 36% of the flow path. Figure 7(a) compares the blade surface velocity on the main blade as calculated by Katsanis and by the present method. Figure 7(b) gives a similar comparison for the splitter blade. The comparisons show generally good agreement. Some of the discrepancy is certainly due to the graphical determination of blade profiles from Kramer's data, although the meridional surface of revolution and the passage height were analytically well defined.

7.4 Water Flow in a Straight-Bladed Radial Turbine Rotor.

Experimental data on both static pressure and relative velocity distribution in a two-dimensional rotor passage have been reported by Cartwright (10). This data permits a check on the calculated fluid properties between blades. Figure 8(a) gives the experimental result for the blade to blade variation of static pressure, approximately half way along the blade chord. The calculated pressure variation gives an excellent estimate of the local pressure gradient although, because of frictional pressure drop, the general level of static pressure in the real flow is somewhat lower than the calculated value. Figure 8(b) shows the variation of relative velocity, W, expressed as a fraction of the blade tip speed U_T. The experimental data was obtained by a quantitative flow visualisation technique. The displacement thickness of the shroud boundary layers has raised the level of velocity observed in the real flow, but once again the computed solution gives a good approximation to velocity gradients.

8. CONCLUSIONS.

By careful choice of the region of solution for the new procedure, techniques have evolved for dealing with multi-bladed turbomachinery applications.

Convergence problems of high subsonic Mach number flow have been overcome without using damping factors, so the need for repeated reruns, seeking suitable damping factors to assist convergence, has never arisen. The axial turbine stator of Section 7.2 exhibited Mach numbers of about 0.85 on one of the blade surfaces, and other solutions (not reported here) have been obtained, without convergence problems, for flow with local Mach numbers only fractionally less than unity. No one technique can be regarded as having provided this high Mach number ability, it is more a combination of the region

of solution, the orthogonal grid and the 'non-iterative' density algorithm. The convergence process of the techniques appears to be extremely stable, and have so far not failed to converge, on both stream function and density, under conditions where the flow is subsonic everywhere.

The numerical methods used in the computation have been tested against exact solutions, and found to give good accuracy. More importantly the procedure has been applied to examples of both compressible and incompressible blade-to-blade flows for which experimental data is available, and has been found to provide a good approximation to the real flow. Improvements to the method, notably in the incorporation of terms to account for shear stress within the fluid, are currently in hand, and considerably more experimental verification is required. The indications are, however, that the procedure in its present form provides a useful guide to the selection of possible blade profiles of a wide range of turbomachines at the design stage.

ACKNOWLEDGEMENT.

The authors wish to acknowledge the support of the Science Research Council, London, in the development of the computational method described in this paper.

9. REFERENCES.

1. HILL, M.J.,
Numerical Solutions for Mixed Flow Turbomachines. Ph.D. thesis, UMIST, 1974.

2. KRAMER, J.J., STOCKMAN, N.O. and BEAN, R.J.,
Non-Viscous Flow Through a Pump Impeller on a Blade-to-Blade Surface of Revolution. NASA TN D-1108, 1962.

3. KRAMER, J.J., STOCKMAN, N.O. and BEAN, R.J.,
Incompressible Non-Viscous Blade-to-Blade Flow Through a Pump Rotor with Splitter Vanes. NASA, TN D-1186, 1962.

4. KATSANIS, T. and McNALLY, W.D.,
Fortran Program for Calculating Velocities and Streamlines on a Blade-to-Blade Stream Surface of a Tandem Blade Turbomachine. NASA TN D-5044, 1969.

5. SMITH, D.L.J. and FROST, D.H.,
Calculation of the Flow Past Turbomachine Blades. Proc. I.Mech.E., 1969-1970, 184, (Pt.3G).

6. STANITZ, J.D.,
Two-Dimensional Compressible Flow in Turbomachines with Conic Flow Surfaces. NACA, Report 935, 1949.

7. AMES, W.F.,
Numerical Methods for Partial Differential Equations, Nelson, 1969.

8. GOSTELOW, J.P.,
Potential Flow Through Cascades - A Comparison Between Exact and Approximate Solutions. A.R.C. C.P. 807, 1964.

9. WHITNEY, W.J., SZANCA, E.M., MOFFITT, T.P. and MONROE, D.E.,
Cold-Air Investigation of a Turbine for High Temperature-Engine Applications. NASA TN D-3751.

10. CARTWRIGHT, W.G.,
The Determination of the Static Pressure and Relative Velocity Distribution in a Two-Dimensional Radially Bladed Rotor. I.Mech.E., Warwick Conference paper C111/73, 1973.

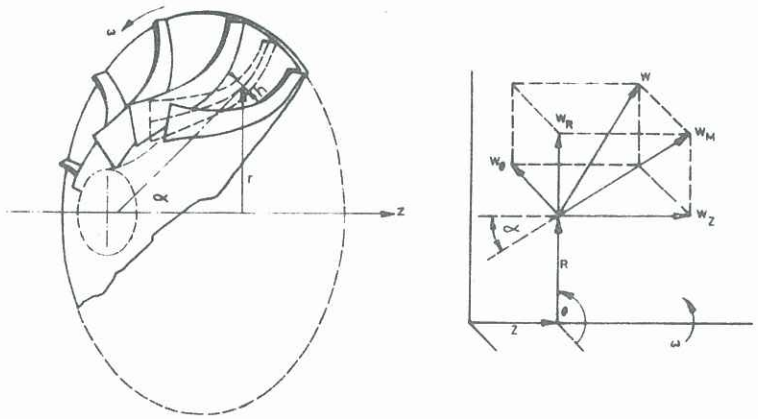

FIG 1 COORDINATE SYSTEM RELATIVE TO BLADES. CENTRE LINE OF FLOW PASSAGE GENERATES A SURFACE OF REVOLUTION

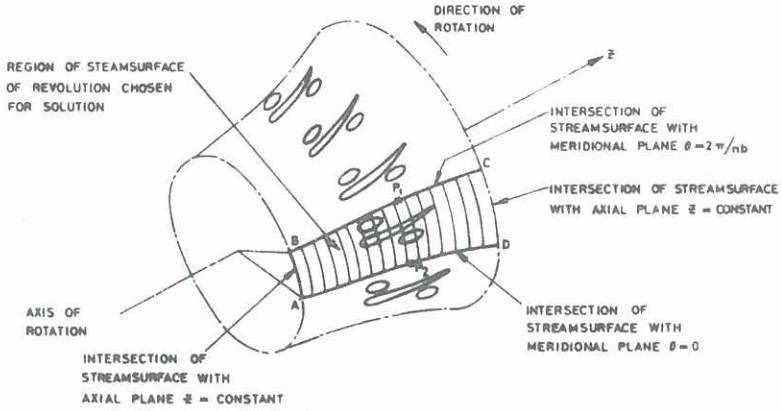

FIG. 2. REGION OF STREAMSURFACE OF REVOLUTION CHOSEN FOR SOLUTION WITH nb SIMILAR CONFIGURATIONS OF OBJECTS

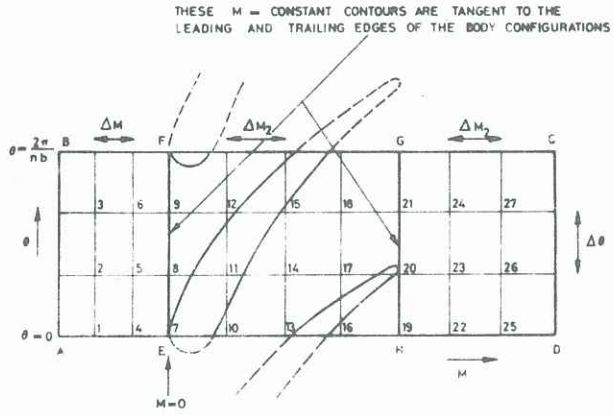

FIG. 3. ILLUSTRATING ORTHOGONAL GRID IN M — θ PLANE

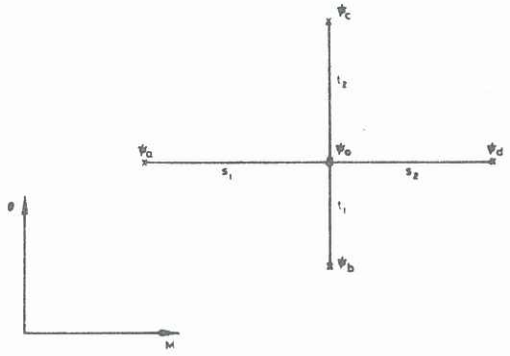

FIG 4 FIVE-POINT MOLECULE USED FOR FINITE-DIFFERENCE APPROXIMATIONS ON ORTHOGONAL M — θ GRID

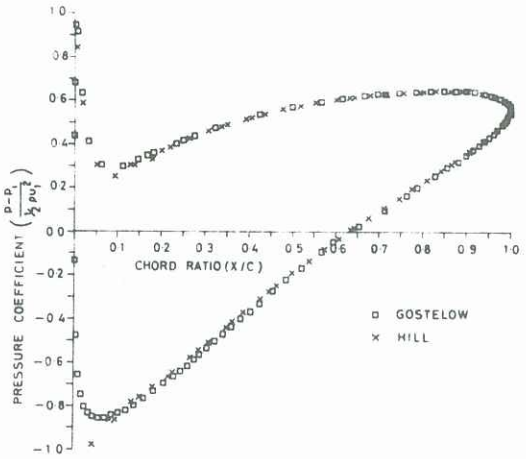

FIG. 5. BLADE SURFACE PRESSURE COEFFICIENT DISTRIBUTION FOR COMPARISON OF GOSTELOW'S ANALYTICAL SOLUTION AND HILL'S FIXED GRID SOLUTION FOR A CASCADE OF AEROFOILS

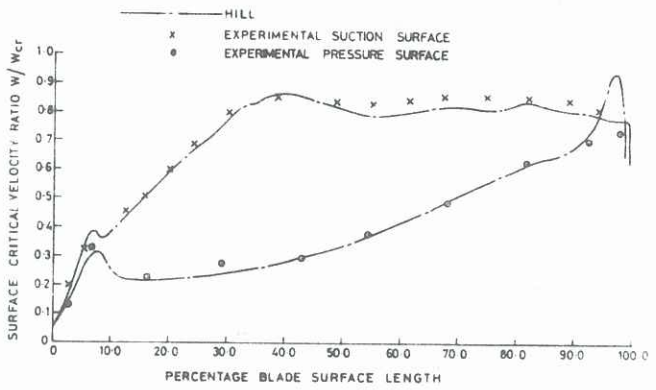

FIG.6. COMPARISON OF BLADE SURFACE VELOCITIES PREDICTED BY THE HILL FIXED GRID METHOD WITH EXPERIMENTAL RESULTS FOR AN AXIAL TURBINE STATOR

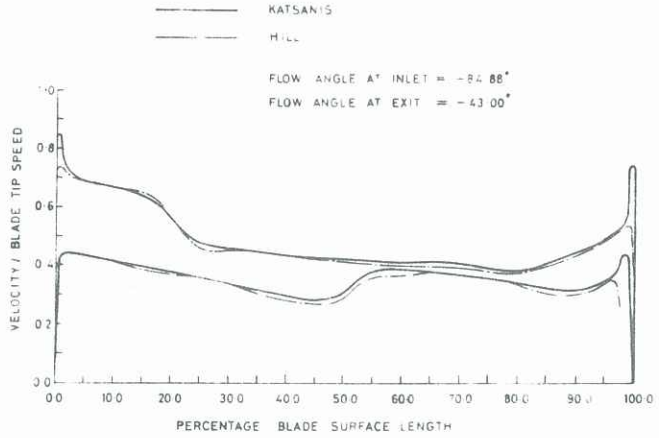

FIG. 7(a). MAIN BLADE VELOCITY DISTRIBUTION FOR COMPARISON OF KATSANIS SOLUTION AND THE HILL FIXED GRID SOLUTION FOR A MIXED FLOW COMPRESSOR WITH SPLITTER VANES.

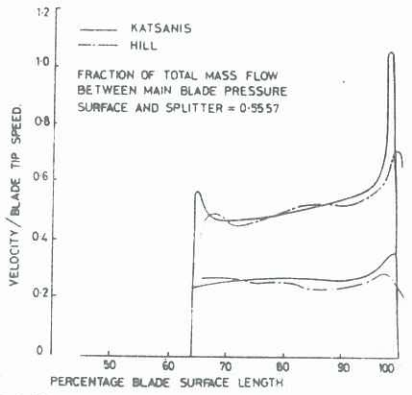

FIG.7(b). SPLITTER BLADE VELOCITY DISTRIBUTION FOR COMPARISON OF KATSANIS SOLUTION AND HILL FIXED GRID SOLUTION FOR A MIXED FLOW COMPRESSOR WITH SPLITTER VANES

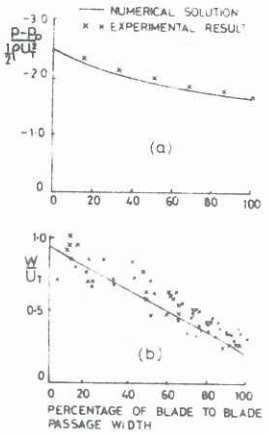

FIG 8. PRESSURE AND VELOCITY VARIATION BETWEEN BLADES, IN A RADIAL TURBINE ROTOR